Broken Bar Detection In Induction Machines Using ADC 42

Krstevski Toni

Abstract – **This study describes broken bar detection in induction motors before actual breakdown occurs in purpose maintenance to be predictable. It is based on sampling stator current on motor with high resolution A/D converter (ADC 42), and three phase current waveforms are analyzed using Fast Fourier Transformers (FFT).**

Key words – **ADC 42, FFT.**

I. Introduction

Squirrel-cage induction motor is low priced, robust and rugged, simple and easy to maintain, it has become the most commonly used electrical rotating machine in industry. So, the need for detection of rotor faults as in rotor bar or in end-ring become increasingly important. Defect in rotor will result in a high resistance which will overheat that area, so cracking or small hale may than occur in rotor bar [4]. It is known that rotor bar and end-ring faults yield asymmetrical operation of induction machines causing unbalanced current, torque pulsation, increased losses and decreased average torque. Vibration analyses, thermal analyses and current spectrum analyses have been applied to monitor rotor bar faults, focusing on current spectrum analyses as the current signal is easily accessible for induction motor. In industry however, low cost and high sensitivity of motor diagnostic system is highly demanded.

II. Model of Asymmetric Rotor of Induction Cage Motor

For the purpose of analyses, each rotor bar and segment of the end ring is replaced by an R-L series equivalent circuit representing the resistive and inductive nature of cage. Such an equivalent circuit is shown at Fig. 1. Assuming the rotor of squirrel- cage induction machine to be symmetric, an equivalent model of a wound - rotor machine may be obtained in synchronously rotating dq reference frame [2] and [3]:

Toni Krstevski is student at SS. Cyril and Methodius University, Faculty of Electrical Engineering, Karpos II bb, P.O.B. 574 1000 - Skopje, Macedonia, E-mail: toni77kr@yahoo.com

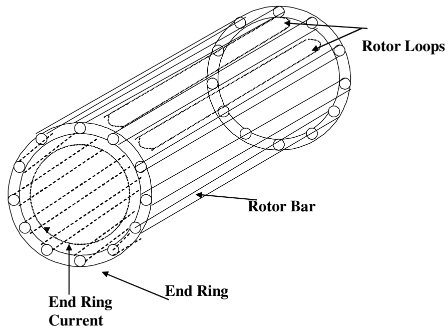

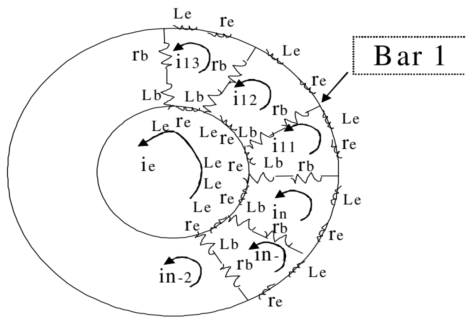

Fig. 1. Rotor cage equivalent circuit

$$v_{ds} = r_s i_{ds}^e + p\lambda_{ds}^e - \omega_e \lambda_{qs}^e \tag{1}$$

$$v_{qs} = r_s i_{qs}^e + p\lambda_{ds}^e + \omega_e \lambda_{ds}^e \tag{2}$$

$$v_{dr} = 0 = r_s i_{dr}^e + p\lambda_{dr}^e - \left(\omega_e - \omega_r\right)\lambda_{qr}^e \tag{3}$$

$$v_{qr} = 0 = r_s i_{qr}^e + p\lambda_{qr}^e - \left(\omega_e - \omega_r\right)\lambda_{dr}^e \tag{4}$$

$$\lambda_{ds}^e = L_{ls} i_{ds}^e + L_m \left(i_{ds}^e + i_{dr}^e\right) \tag{5}$$

$$\lambda_{qs}^e = L_{ls} i_{qs}^e + L_m \left(i_{qs}^e + i_{qr}^e\right) \tag{6}$$

$$\lambda_{dr}^e = L_{lr} i_{dr}^e + L_m \left(i_{ds}^e + i_{dr}^e\right) \tag{7}$$

$$\lambda_{qr}^e = L_{lr} i_{qr}^e + L_m \left(i_{qs}^e + i_{qr}^e\right) \tag{8}$$

Where:
P- Number of poles;
w_r -rotor speed;
T_e -torque;
r_s - equivalent stator resistance;
r_r - equivalent rotor resistance;
L_{ls} - equivalent stator leakage inductance;
L_{lr} - equivalent rotor leakage inductance;
L_m - equivalent magnetizing inductance;

In many studies such as the work of Krause [5], is convenient to express the voltage and flux linkage equations from Eq. (1) to Eq. (8) in terms of reactance. From this studies determination of torque, in synchronously rotating reference frame is made with neglect the time rate of change of all flux linkages and then employ the relationships:

$$\sqrt{2}\,\tilde{F}_{as} = F_{qs}^{e} - jF_{ds}^{e} \tag{9}$$

$$\sqrt{2}\,\tilde{F}_{ar} = F_{qr}^{'e} - jF_{dr}^{e} \tag{10}$$

Torque can be expressed in terms of currents in phasor form by first writing the torque in terms of currents in the synchronously rotating reference frame and utilizing Eq. (9) and (10) to relate synchronously rotating reference frame and phasor quantities. The torque expression becomes:

$$T_e = 3\left(\frac{P}{2}\right)\left(\frac{X_m}{\omega_b}\right)R_e\left[j\tilde{I}_{as}^{*}\tilde{I}_{ar}^{'}\right] \tag{11}$$

where:

ω_b is base electrical angular velocity used to calculate the inductive reactances;

$\tilde{I}_{as}^{*}$ is the conjugate of $\tilde{I}_{as}$;

The vast majority of singly excited machines are the squirrel cage rotor type, where :

$$\tilde{I}_{ar}^{'} = -\frac{j(\omega_e/\omega_b)X_m}{r_r^{'}/s + j(\omega_e/\omega_b)X_{rr}^{'}}I_{as}^{'} \tag{12}$$

where:

$$X_{rr}^{'} = X_{lr}^{'} + X_m \tag{13}$$

Substituting Eq. (12) into Eq. (11), yield:

$$T_e = \frac{3\left(\frac{P}{2}\right)\left(\frac{\omega_e}{\omega_b}\right)\left(\frac{X_m}{\omega_b}\right)\left(\frac{r_r^{'}}{s}\right)\left|\tilde{I}_{as}\right|^2}{\left(\frac{r_r^{'}}{s}\right)^2 + \left(\frac{\omega_e}{\omega_b}\right)^2 X_{rr}^{'2}} \tag{14}$$

where the slip s is defined:

$$s = \frac{\omega_e - \omega_r}{\omega_e} \tag{15}$$

In general all n-loop rotor current (i_{l1}, i_{l2},..., i_{ln}) are mapped into a n-dimensional vector space. This new space vector is defined by the transformation matrix T such that:

$$\begin{bmatrix} i_{r1}^{'} \\ i_{r2}^{'} \\ i_{rn}^{'} \end{bmatrix} = T\begin{bmatrix} i_{l1}^{'} \\ i_{l2}^{'} \\ i_{ln}^{'} \end{bmatrix} \tag{16}$$

where:

$i_{r1}^{'}$ - real part of the rotor current space vector;
$i_{r2}^{'}$ - imaginary part of the rotor current space vector;
$i_{r3...rn}^{'}$ - zero sequence components of the rotor current space vector;

$$\begin{bmatrix} f_d \\ f_q \\ 0 \\ . \\ . \\ . \\ 0 \end{bmatrix} = \frac{n-1}{n}\begin{bmatrix} \cos(\theta) & . & . & . & \cos\left(\theta + \left\{\frac{n-1}{n}\right\}2\pi\right) \\ \sin(\theta) & . & . & . & \sin\left(\theta + \left\{\frac{n-1}{n}\right\}2\pi\right) \\ . & . & . & . & . \\ . & . & . & . & . \\ . & . & . & . & . \\ Z_{n1} & . & . & . & Z_{nn} \end{bmatrix}\begin{bmatrix} f_1 \\ f_2 \\ . \\ . \\ . \\ f_n \end{bmatrix} \tag{17}$$

The T transformation is generated from a very simple algorithm. The first two lines from Eq. (17) correspond to n-phase dq transformation, plus a constant. Since the vectors formed by the two lines are linearly independent, the null space of this 2xn sub-matrix has a dimension (n-2). A base for the null space is defined by (n-2) linearly independent vectors $\underline{Z}$ such that $T_{dq}\cdot\underline{Z}=0$. Taking θ equal to zero, for simplicity:

$$\begin{bmatrix} 1 & \cos\left(\frac{2\pi}{n}\right) & . & . & . & \cos\left(\frac{n-1}{n}2\pi\right) \\ 0 & \sin\left(\frac{2\pi}{n}\right) & . & . & . & \sin\left(\frac{n-1}{n}2\pi\right) \end{bmatrix}\begin{bmatrix} z_1 \\ z_2 \\ . \\ . \\ . \\ z_n \end{bmatrix} = 0 \tag{18}$$

From [1], [2] and [3]:

$$\begin{bmatrix} z_1 \\ z_2 \end{bmatrix} = \begin{bmatrix} 1 & \cos\left(\frac{2\pi}{n}\right) \\ 0 & \sin\left(\frac{2\pi}{n}\right) \end{bmatrix}^{-1} \times \begin{bmatrix} \cos\left(\frac{2}{n}\cdot 2n\right) & . & . & . & \cos\left(\frac{n-1}{n}\cdot 2\pi\right) \\ \sin\left(\frac{2}{n}\cdot 2\pi\right) & . & . & . & \sin\left(\frac{n-1}{n}\cdot 2\pi\right) \end{bmatrix}\cdot\begin{bmatrix} z_3 \\ . \\ . \\ z_n \end{bmatrix} \tag{19}$$

z_3, z_4,..., z_n, can be arbitrary chosen. Making z_3=1 and z_4= z_5=... z_n=0 z_{31} and z_{32} are determined, resulting in third vector of the null space:

$$\begin{bmatrix} z_{31} & z_{32} & 1 & 0 & . & . & . & 0 \end{bmatrix} \tag{20}$$

Taking z_4=1 and z_3= z_5=... z_n=0 z_{41} and z_{42} are determined, and the fourth vector of hull space is calculated as:

$$\begin{bmatrix} z_{41} & z_{42} & 0 & 1 & . & . & . & 0 \end{bmatrix} \tag{21}$$

The rotor current complex vector ($\underline{i}_r$) is computed from the symmetric model. With i_r referred to a rotor fixed reference frame, the n- loop currents (i_{li}) are then computed as:

$$\begin{bmatrix} i_{l1} \\ i_{l2} \\ i_{l3} \\ i_{ln} \end{bmatrix} = T^{-1}\begin{bmatrix} i_{dr} \\ i_{qr} \\ 0 \\ 0 \end{bmatrix} \tag{22}$$

Let assume that kith bar is broken. The null current through this bar is obtained by modifying the n-loop rotor current vector according to:

$$\begin{bmatrix} i_{l1}^{new} \\ i_{l2}^{new} \\ . \\ . \\ . \\ i_{lk}^{new} \\ i_{l(k+1)}^{new} \\ . \\ . \\ . \\ i_{ln}^{new} \end{bmatrix} = T \begin{bmatrix} i_{l1} \\ i_{l2} \\ . \\ . \\ . \\ \frac{i_{lk} + i_{l(k+1)}}{2} \\ \frac{i_{lk} + i_{l(k+1)}}{2} \\ . \\ . \\ . \\ i_{ln} \end{bmatrix} \tag{23}$$

III. INSTRUMENT DESCRIPTION

According on mathematical model that is represented above for the expectation is to have increasing of the amplitude of sideband components, while other harmonics maintained their amplitude when some bar of the squirrel - cage induction motor is broken. For the purpose to show that, stator current is measured on the terminals of the motor with broken bar and FFT analyses are made. Analog to digital converter is used (ADC 42) that is shown on Fig. 2, with characteristic which are given in Appendix I.

Fig. 2. Analog to digital converter (ADC 42)

For measuring stator current of the motor is used digital clump meter, shown on Fig. 3 which pick up the current flowing through the conductor. Technical specifications of clump meter are given in Appendix II.

Fig. 3. Digital clump meter

Because measured current on transformer jaws is with small velocity it was necessary to amplify the signal so the ADC 42 could measured. An electronic device as amplifier was made and its electronic circuit is given at Appendix III.

IV. EXPERIMENTAL RESULTS

It was used 3 phase induction motor from SIEMENS type 1LA 3106-4AA21-Z with characteristics that are given in Appendix IV. Also, Pico Scope Software application [6] is used. Fig. 4. shows the current frequency spectrum with the motor in healthy conditions. Some harmonics are visible in the measured current spectrum, with emphasis on the third, fifth and seventh harmonics, caused by inherent asymmetries of three phase windings. Besides that, the sideband component at frequency $(1\text{-}2s)f_e$ can also be seen, which is caused by inherent asymmetries of the cage. Fig. 5. shows the harmonic current spectrum for broken bar. It is notorious the increase in the amplitude of the sideband components, while other harmonics components maintained their amplitudes. Fig. 6. shows the broken bar of the squirrel - cage of induction motor.

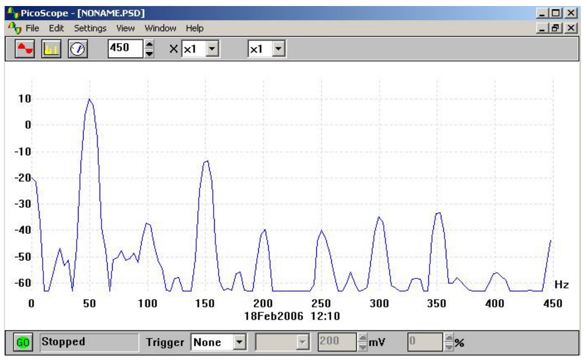

Fig. 4. Current frequency spectrum with motor in healthy conditions

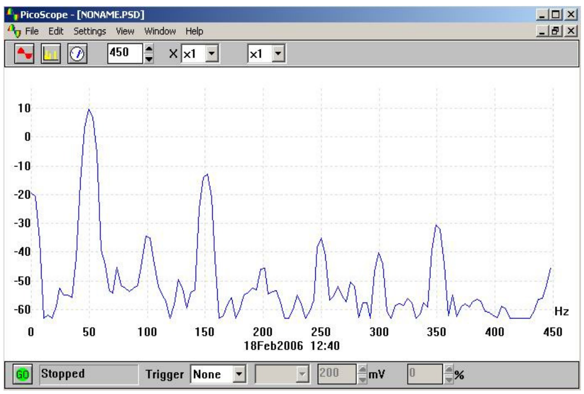

Fig. 5. Current frequency spectrum with broken bar

Fig. 6. Broken bar of squirrel cage of induction motor

V. Conclusion

In this paper, is given mathematical model of classical fourth-order transient model of symmetrical induction machines, with additional computation limited to the transformation of the rotor current vector to a rotor fixed reference frame. Also are made measurement on stator current on motor with healthy conditions and with a broken bar. Experimental results show increasing of amplitude of sidebands components and theoretical mathematical model confirm that.

Appendix I

ADC 42 Characteristic

Resolution 12 bits; Channels 1 x BNC; Voltage ranges ±5 V; Overload protection ±30 V; Input impedance 1 MΩ; Sampling rate 15 kS/s; Accuracy ±1%; Scope time bases 500 µs/div to 50 s/div; Spectrum ranges 0 to 7kHz, 65 dB dynamic range; Analog bandwidth 7.5 kHz; Buffer Size- No buffer**;** Power supply-Not required; Dimensions 55x55x15mm (2.17x2.17x0.6 in); Output connector D25 to PC parallel port; Supplied software Pico Scope; DOS and Windows (3.x, 95/98/XP, NT/2000);

Appendix II

Technical specification of Clump meter

- Max. Voltage between terminals and earth ground: 600 Vrms,
- Operating principle: dual slop integration,
- Sample rate: 2 times/ sec for digital data;

Appendix III

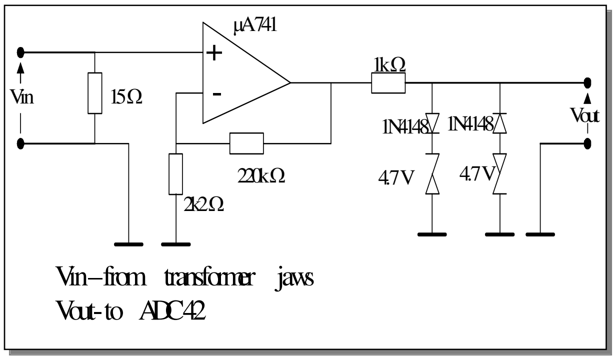

Appendix IV

3 phase squirrel-cage induction motor from Siemens, type: 1LA 3106-4AA21-Z; IEC 100L;

Nr. E6482 1169 04 012; B5 IP 54; Rot KL16; 220/380 V; Δ/Y; 9/5.2A; 2.2 kW; ICL B cosφ 0.82 ; 1415/min; 50Hz; VDE 0530

References

[1] Carla C. Martines Cunha, Renato O. C. Lyra, Braz J. Cardaso Filho, "Simulation and Analysis of Induction Machine with rotor Asymmetries" *IEEE Transaction on industry applications,* Vol. 41, pp 18-24, No. 1, January/ February 2005

[2] Alfredo R. Muňoz, Thomas A. Lipo, "Complex Vector Model of the Squirrel-Cage Induction machine Including Instantaneous Rotor Bar Current" *IEEE Transaction on industry applications,* Vol. 35, pp 1332-1339, No. 6, November/ December (1999)

[3] Elkasagby, N. M., Eastham, A. R. and Dawson, G. E. "Detection of broken bar in the Cage rotor on an Induction Machine" *IEEE Transaction on Industry application,* Vol. 28, No. 1, pp 165-171 (1992)

[4] Hakan Çaliş, Abdülkadir Çakir, Müslüm Arkan, "Sensorless broken bar detection in induction machines" eleco.emo.org.tr/eleco2003/ELECO2003/asession/A2-05.pdf

[5] P.C. Krause, O. Wasynezuk, S.D. Sudhoff, "Analysis of the electrical machinery" *The institute of electrical and electronics engineers,* pp New York, 1995

[6] http://www. pico tehnology.com